Journal of Alloys and Compounds 884 (2021) 161071

Contents lists available at ScienceDirect

Journal of Alloys and Compounds

journal homepage: www.elsevier.com/locate/jalcom

Flexible lead-free NBT-BT/PVDF composite films by hot pressing for low-energy harvesting and storage

M. Vijatovic Petrovic[a,*], F. Cordero[b], E. Mercadelli[c], E. Brunengo[d], N. Ilic[a], C. Galassi[c], Z. Despotovic[e], J. Bobic[a], A. Dzunuzovic[a], P. Stagnaro[d], G. Canu[f], F. Craciun[b]

[a] Institute for multidisciplinary research, University of Belgrade, Kneza Viseslava 1, 11 000 Belgrade, Serbia
[b] CNR-ISM, Istituto di Struttura della Materia, Area della Ricerca di Tor Vergata, Via del Fosso del Cavaliere, 100, I-00133 Rome, Italy
[c] CNR-ISTEC, Istituto di Scienza e Tecnologia dei Materiali Ceramici, Via Granarolo 64, I-48018 Faenza, Italy
[d] CNR-SCITEC, Istituto di Scienze e Tecnologie Chimiche "Giulio Natta", Via de Marini 6, 16149 Genoa, Italy
[e] Institute Mihajlo Pupin, Volgina 15, 11000 Belgrade, Serbia
[f] CNR-ICMATE, Istituto di Chimica della Materia Condensata e di Tecnologie per l'Energia, Consiglio Nazionale delle Ricerche, Via de Marini 6, 16149 Genoa, Italy

ARTICLE INFO

Article history:
Received 16 April 2021
Received in revised form 29 June 2021
Accepted 4 July 2021
Available online 6 July 2021

Keywords:
Composite materials
Polymers
Piezoelectricity
Energy storage materials
Energy harvesting

ABSTRACT

The idea of this work is finding the way to efficiently and safely use mechanical energy released in small quantities around us to power up small-scale electronic devices used in everyday life. To this purpose, flexible lead-free piezoelectric composite films were prepared by hot pressing. Different amounts (30, 35 and 40 vol%) of lead-free piezoelectric material bismuth sodium titanate-barium titanate were embedded in the matrix of polyvinylidene fluoride under carefully optimized conditions of temperature and pressure, obtaining flexible films with quite homogeneous distribution of piezo-active filler. ATR-FTIR analysis revealed that hot pressing the flexible films caused a transformation of electro-inactive PVDF α-phase into electro-active β and γ phases. Dielectric measurements showed an increase of the permittivity up to 80 with the active phase increasing. Anelastic measurements showed that the elastic modulus increases as well with the fraction of active ceramic phase. Lastly, obtained flexible polymer-composites demonstrated notable properties both for energy storage and energy harvesting application, showing up to 74% of energy storage efficiency and, from testing of the force impact, up to 9 V and ~ 80 μW of output voltage and power.

1. Introduction

An important task of the scientific community is to find the way of using the enormous amount of mechanical energy released through the vibrations in everyday life, e.g. by human walking, transportation movement, sound waves etc. as a renewable and safe energy source. The perspective of exploiting the mechanical energy of the surrounding environment can have a huge influence on our daily life. In this way, many of the health controlling devices, safety devices, sensors, alarms, lights and other small devices could be powered completely independently from external electricity sources (such as electricity grid and batteries), thus highly reducing our dependence from them as well as our total energy consumption. Piezoelectric generators have great potential for powering low-power portable devices and self-powered electronic systems by extraction of mechanical energy. The advantage of the piezoelectric mechanism over other conversion mechanisms lies in its high energy density and scalability across a wide range of sizes. Thus far piezoelectric generators commercially available are mostly lead-based materials. These materials based on lead-zirconate titanate (PZT) have shown the best piezoelectric performance in many commercial applications [1–11]. However, the family of lead-based materials is now facing the challenge due to its environmental incompatibility. There is a urgent need for lead-free substitutes that can have piezoelectric properties comparable to the ones obtained from the lead-containing materials [12].

During previous investigations, barium titanate (BT) and sodium bismuth titanate (NBT) based materials synthesized in specific compositions, have shown to be among lead-free piezoelectrics with the highest d_{33} coefficients for possible replacement of PZT [2,12–21]. Specifically, the NBT is a piezoelectric material with high remnant polarization at room temperature [13,22,23]. The main obstacle to its application is that it possesses high coercive field and conductivity, preventing easy poling process necessary for good piezoelectric performance. In order to overcome this problem,

* Corresponding author.
E-mail address: miravijat@yahoo.com (M. Vijatovic Petrovic).

https://doi.org/10.1016/j.jallcom.2021.161071
0925-8388/

different solid solutions have been developed during recent years [12,13,17,23]. Solid solution with barium titanate, (1-x)[($Bi_{0.5}Na_{0.5}$)TiO_3]-x$BaTiO_3$ have drawn significant attention due to the existence of a morphotropic phase boundary (MPB) region by simultaneous presence of rhombohedral and tetragonal phases for x about 0.06–0.07 [24,25]. It was detected that in this narrow MPB region (6–7% BT), NBT-BT exhibits enhanced performance. Besides prominent values of remnant polarization this ceramic is known for its great value of dielectric permittivity [23–26].

A recent challenge in electronics is also the utilization of flexible devices with the ability to bend into diverse shapes, which expands the applications of modern electronic devices in different areas. At the same time, polymer-based composites provide the advantages of being flexible, versatile, lightweight, low cost, and able to conform to complicated shapes, while typically involving low-temperature fabrication processes [2–7,9–11,22]. Flexibility of electronic devices based on composites made of a lead-free piezo-active phase embedded in a polymer matrix will enable easy implementation in clothing, shoes and other accessories. Non-toxicity, impressive flexibility and biocompatibility make them a very good choice also for wearable electronics [27–29].

The polyvinylidene fluoride (PVDF) is the polymer matrix of choice for these applications. Flexible composites based on PVDF can be prepared by solvent casting, melt blending and/or molding methods. Taking into account the relatively low melting temperature of this polymer (~180 °C), a smart way of flexible films preparation was here developed by designing a set up for hot pressing and preparation of flexible films based on PVDF polymer matrix. The hot pressing method was preferably used in order to avoid solvents that are usually used for PVDF dissolution, like dimethylformamide (DMF) [30–32]. This simple but rarely exploited concept of making flexible composites has attracted significant interest of science community since the process is facile and cost-effective [33–35]. The PVDF polymer is a material with pretty complex molecular and crystalline structure and its properties are highly dependent on the heterogeneity of the system itself. It is indeed a semi-crystalline material with five polymorph crystalline phases that are defined by the conformation of the polymer chains [31,33,34]. The α-phase shows no polarity, it does not possess piezo- and pyroelectric properties, hence neither ferroelectric properties but the other polymorphs β, γ and δ are polar. The most preferable is the electroactive β-phase, which shows high polarity, high spontaneous polarization and piezoelectric coefficient (13–28 pC/N) [31–34]. The PVDF molecular interactions are governed by the short-range Vander-Waals forces and hence low potential barriers for the rotation of chain molecules enable easy conversion between the polymorphs. Slightly more stable is the non-polar α-phase in comparison with the polar β-phase [33–35]. Literature data have already shown that the ferroelectrically inactive α-phase of PVDF can be converted into electroactive phases β and/or γ by pressing, stretching at elevated temperatures, uniaxial tension, electrical poling, annealing, compression molding etc. [31,34,39–43]. This indicates the possibility of the co-existence of different polymer phases in the material at the same time, which influences the electrical properties of the material as well as potential applications. Chu et al. also demonstrated that by combining non-polar and polar crystalline modifications of PVDF, very high energy density can be achieved, which is notably important for the energy storage application [44]. Moreover, inclusion of fillers in the polymer matrix and formation of polymer composites may enable the nucleation of electroactive β-phase. Some authors have shown that inclusion of barium titanate can make the β-phase to nucleate predominantly, but this process is dependent on the filler size [31,38]. Others evidenced that addition of $NiFe_2O_4$ and $CoFe_2O_4$ in a certain percentage can guarantee the formation of 90% of β-phase. It was explained that CH_2 bonds of PVDF and negatively charged ferrites surface have strong interactions, which induce the formation of all trans conformation with consequent β- crystallographic phase stabilization [31]. There are studies where, along with the addition of the filler (e.g. barium titanate), stretching was performed in order to obtain mainly β-phase in the material [35]. It has been shown that also the poling process has an effect on the phase conversion [42,43].

This research was focused on the preparation of flexible composite films, by combining a highly flexible PVDF polymer matrix with lead-free piezoelectric perovskites, 0.94[($Bi_{0.5}Na_{0.5}$)TiO_3]–0.06$BaTiO_3$ (NBT-BT), in different ratios. Since, to the best of our knowledge, a rather limited number of papers dwelled with these particular composites, a crucial point of this investigation is to show that this material is quite versatile and possesses functional properties which are sensitive to both microscopic and chemical modifications [45,46]. All the evidences reviewed above show that proper tailoring of material properties is possible by selecting adequate polymer and filler pairs, which combined with the choice of a suitable processing method will allow the improvement of existing and the widening of the potential applications. Using a lead-free piezoelectric polymer-based composite material for low-energy harvesting and energy storage for always-on devices paves the way to a new type of safe production and usage of energy for everyday life.

2. Experimental

2.1. Preparation of active phase powders and flexible composite films

Powders of 0.94[($Bi_{0.5}Na_{0.5}$)TiO_3]–0.06$BaTiO_3$ were synthesized by solid state route. The stoichiometric amounts of $BaCO_3$ (99.0%, Merck), TiO_2 (99.9%, Degussa), Na_2CO_3 (99.5%, Merck), Bi_2O_3 (99.9%, Aldrich) were ball milled in ethanol for 48 h using a polyethylene jar and zirconia milling media of different diameters. The milling media/ precursors powder weight ratio was fixed at 1.5. The dried precursors mixture was then sieved at 250 μm and calcined at 800 °C for 1 h. The calcined NBT-BT powder was finally ball milled in ethanol for 120 h, dried and sieved at 250 μm. The preparation process has been optimized in order to obtain a highly reactive perovskite phase, able to guarantee optimal piezoelectric properties of the resulting ceramics [25,47].

Commercial PVDF powder (Alfa Aesar) and the previously synthesized NBT-BT powders were mixed in three different ratios: namely, 30, 35 and 40 vol% of NBT-BT powders. Samples were named according to the amount of filler as NBT-BT/ PVDF 30/70, NBT-BT/ PVDF 35/65 and NBT-BT/PVDF 40/60, respectively. The powder of the active phase was mixed with PVDF powder in the isopropanol with applied ultrasound probe. Mixture was dried in the furnace at 60 °C. The samples have been further subjected to a hot-pressing process using a custom built set up. The hot pressing procedure consisted of heating up to 190 °C with holding time of 10 min while the pressure of 5 MPa was applied at 160 °C and released at 160 °C during natural cooling.

2.2. Characterization of powders and composite films

XRD analysis of NBT-BT powders and composite films was carried out using a Bruker D8 Advance X-ray Diffractometer and Rigaku MiniFlex 600 instrument, respectively. Particles morphology was observed with a LEO 1450VP (LEO Electron Microscopy Ltd) SEM microscope, while composites morphology was investigated by a Tescan VEGA TS 5130MM instrument. Both the external surface and transversal section (obtained by fracture of the samples) of the composite films were observed.

Infrared spectroscopy measurements on the composites were carried out in attenuated total reflectance (ATR) mode by a PerkinElmer Spectrum Two™ FTIR spectrometer and collecting spectra in the 4000–400 cm^{-1} range. Eq. (1) was used to estimate the

relative fraction of the electroactive phase(s) (F_{EA}) on normalized spectra, subtracted from the contribution of the filler [32,48,49]:

$$F_{EA} = \frac{I_{EA}}{1.26I_{\alpha} + I_{EA}} * 100 \quad (1)$$

where I_{EA} is the absorbance of the band at about 840 cm^{-1} that can be assigned to β and/or γ phase, I_{α} the absorbance of a characteristic band of the α phase and 1.26 the ratio between the absorption coefficients at the respective wavenumbers. As suggested by X. Cai et al. [50], when β and γ phases were present simultaneously, the peak-to-valley height ratio between the two peaks around 1275 and 1234 cm^{-1} was used to separate the two contributions (F_{β}) and (F_{γ}).

The crystallinity degree (X_C) of neat PVDF and composites was evaluated by differential scanning calorimetry (DSC). Two repeats per sample were performed with a Mettler DSC 821^e instrument, heating from room temperature up to 220 °C at a scan rate of 10 °C/min under N_2. X_C values were calculated as the ratio between the measured enthalpies (ΔH_m), normalized with respect to the actual content of PVDF in the composite, and enthalpy of fusion of a perfect PVDF crystal (ΔH_0 = 104.6 J/g) [39].

The relative density of the composites was calculated as the percentage ratio between the measured density (by Archimedes' method) and the calculated theoretical density. The latter was calculated as in [41], using the appropriate volume fraction of filler, crystallinity degree, and relative amount of electroactive phases of PVDF. A filler density of 5.965 g/cm^3, as measured by a Micrometrics Instrument Corporation AccuPycTM 1330 helium pycnometer, was used.

Optical properties of the prepared systems were investigated in the wavelength range 200–1400 nm using a Shimadzu 2600 UV–VIS spectrophotometer.

For dielectric, ferroelectric and anelastic characterizations silver electrodes (6 mm in diameter) were painted on the films (PEMCO silver paint, with organic solvent, Alfa Aesar). Dielectric measurements were carried out in the temperature range 100–430 K and frequency range 0.2 kHz - 1 MHz with an HP4284A meter, by using a four wire probe. Samples were placed in a modified Linkam HFS600E-PB4 stage during heating and cooling at 1.5–2 K/min. Anelastic measurements were performed in the temperature range 130–400 K by measuring the complex dynamic Young's modulus $E = E' + iE''$ in the kHz range with the free flexural resonance method [51,52]. Strips about 30 mm long were cut from the films, suspended on two thin thermocouple wires in high vacuum or 0.1 mbar He below room temperature and electrostatically excited on their flexural modes. The strips were made conductive with silver paint in correspondence of the electrode and for shorting the thermocouple. At least the 1st and 3rd modes could be alternately excited during the same experiment, probing two or more frequencies in the ratio 1:5.4 and higher [52]. For ferroelectric characterization a Precision Multiferroic Test System with High Voltage Interface-Radiant Technologies, Inc. was employed up to 4000 V. The polarization curves were measured at different external electric fields.

2.3. Poling, film assembly and testing

Electrical poling of the samples was performed in a silicon bath at 135 °C for 40 min and cooled down to 50 °C under the electrical field of 50 kV/cm in the parallel plate configuration. Poled flexible films with 1.5 cm^2 area, were wired and integrated in the Kapton tape (polyimide film) flexible cover as an insulation and protection layer. Since it remains stable under the wide range of temperatures −269 - +400 °C and has a high isolation ability, Kapton is usually used in the flexible electronic industry, for aircrafts, spacecrafts etc. Testing on force impact of 250 N was carried out using Quartz Impulse hammer with IEPE output modal, KISTLER, Italy.

3. Results and discussion

3.1. Characterization of active phase powders

The formation of the NBT-BT perovskite structure has been assessed by the X-ray diffraction (XRD). The XRD pattern reported in Fig. 1a shows that the powder after calcination is mainly composed by NBT-BT (with 4% BT JCPDS 74–9529), crystalized into rhombohedral crystal structure with space group R3c, and traces of un-reacted BT phase (JCPDS 66–0829). The use of highly reactive powders (instead of fully-reacted powders obtained from the corresponding crushed ceramics) has been already successfully proposed for the production of NBT ceramics [47] or NBT-BT/PVDF composites [46]. The average crystallite size of the synthesized powders is 31 ± 1 nm, calculated by the FWHM using the Debye-Scherrer equation. The particles of NBT-BT powders used for the preparation of composite flexible films were morphologically characterized by scanning electron microscopy (SEM). The Fig. S1 displays two SEM images of NBT-BT particles, where aggregates of particles with size prevalently around 100–130 nm can be observed.

3.2. Characterization of composite NBT-BT/PVDF flexible films

One of the prepared NBT-BT/PVDF films is presented in the photograph of Fig. 1c. All the flexible films were in the shape of disks with diameter around 3–4 cm and showed good flexibility. As the amount of inorganic active phase in the polymer matrix increases the film becomes less flexible, as expected.

Morphological SEM analysis of the NBT-BT/PVDF flexible films was carried out. SEM micrographs of the external surface and transversal internal surface of the sample NBT-BT/PVDF 35/65 are reported in Fig. 1b. The following trend was observed, the lower the NBT-BT content, the more uniform the distribution of the filler is. In each film, small areas with predominantly PVDF polymer phase were noticed (Fig. S2 and S3). The thickness of the films can be also determined from the micrographs and ranges from 110, 150 and 200 μm respectively with the increase of active component concentration in the film.

In order to investigate the influence of the hot pressing method on phase composition in PVDF, for comparison, neat PVDF film was also prepared by this method. XRD results of neat PVDF film were compared with the results of commercial PVDF powder, used for the preparation of flexible films (Fig. 2a). The PVDF powder is mainly composed of α-phase, as evidenced by three diffraction peaks at 17.7, 18.4 and 20.0, corresponding to (100), (020) and (110) reflections of the monoclinic α-phase crystals (JCPDS #042–1650), respectively. Additionally, α-phase presents a peak at 2θ = 26.65° corresponding to the (021) diffraction plane. On the other hand, XRD of the neat PVDF flexible film, besides these three peaks, possesses a peak at 2θ = 20.8° which is relative to the sum of the diffraction at (110) + (200) planes of the orthorhombic β-phase (JCPDS #042–1649), proving that the appearance of the β-phase was induced by the hot pressing procedure. The reflections of γ-phase, as detected by IR and DSC analyses discussed in the following, are covered by those of the other polymorphs.

This was an indication that electroactive polymeric phases could be present in the composite films and therefore investigation on the relative amount of PVDF polymorphs was conducted for all flexible composite films [53].

Since, XRD is more sensitive to the inorganic filler, which would largely cover the polymer signal, infrared spectroscopy was found to be a very useful and precise technique to study the polymorphism of the PVDF matrix. It also allows individuation and quantification of the most important crystalline phases [39]. The ATR-FTIR analysis (Fig. 2b–d) confirms and complements the XRD results. The PVDF powders are indeed characterized by a neat predominance of the

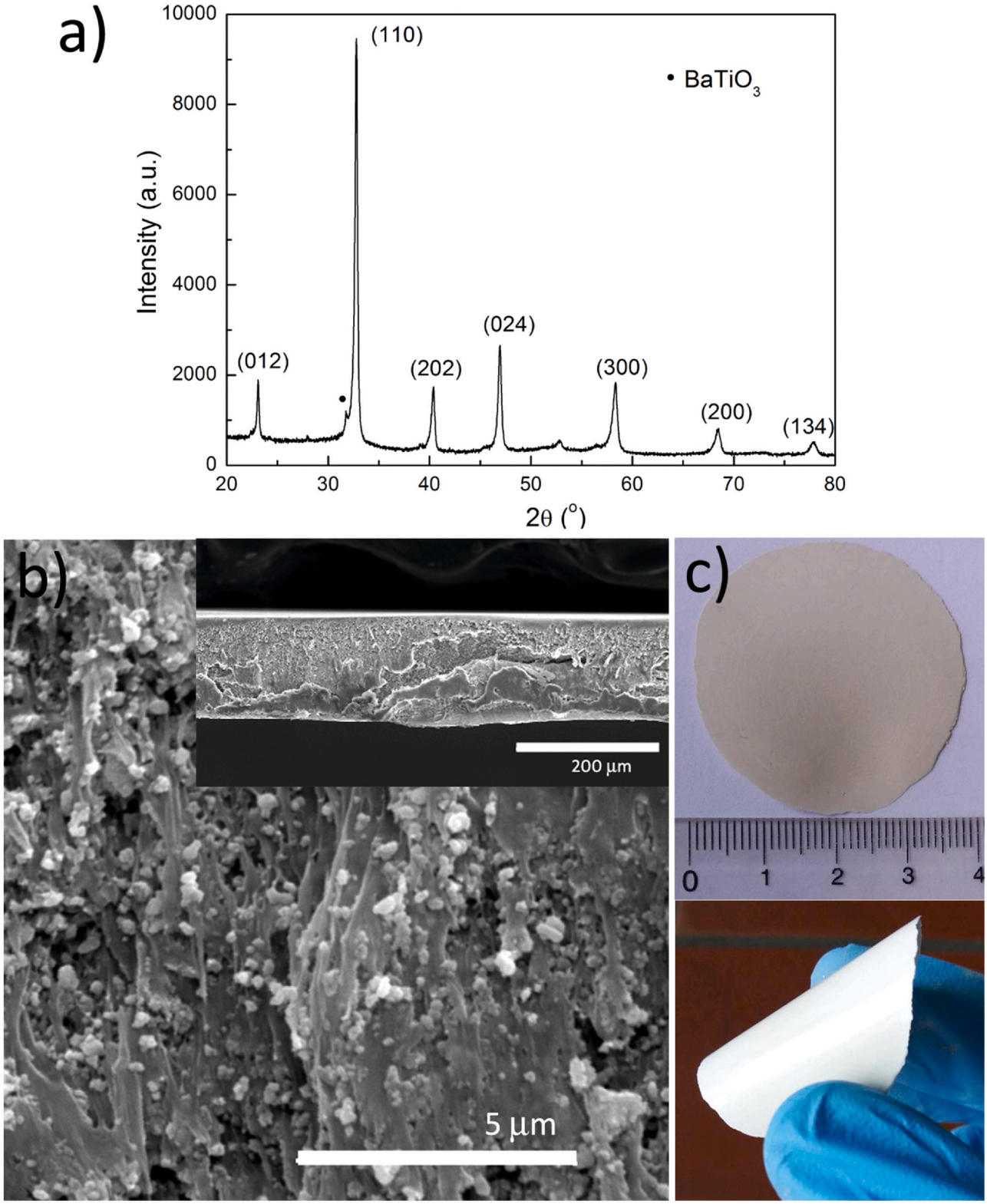

Fig. 1. a) XRD of the NBT-BT powder, calcined at 800 °C x 1 h, used for flexible films preparation, b) SEM representing surface of the film, inset SEM of the transversal internal surface of the film c) Flexible film NBT-BT/PVDF 35/65.

α phase, where the principal peaks characteristic of this non-polar polymorph at 1423, 1383, 1209, 1149, 975, 854, 795, 763, 614, 532, 489, and 410 cm^{-1} are clearly visible. The processing of the polymer induces the formation of electroactive phases, indicated by the peaks around 840 cm^{-1} in the spectrum of the PVDF hot pressed film; the co-presence of the bands at 811 and 1234 cm^{-1}, ascribed to the γ-phase, and those at 443 and 1275 cm^{-1}, exclusive of the β-phase suggests that both the polar polymorphs are simultaneously present.

Also, all the flexible NBT-BT/PVDF composites were subjected to spectroscopic characterization. The broad band around 525 cm^{-1},

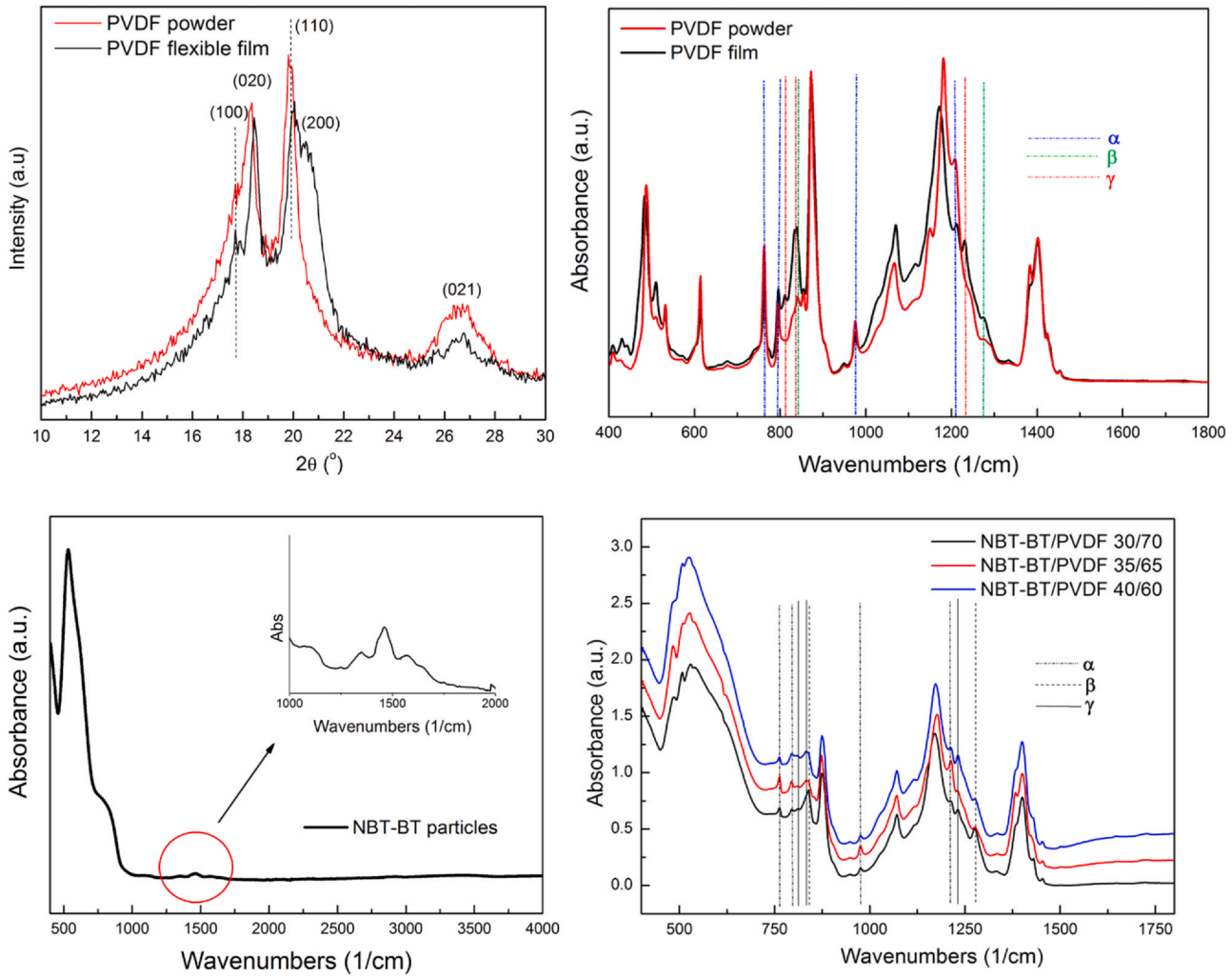

Fig. 2. a) XRD pattern for PVDF powder and neat PVDF film, b) FT-IR spectrum of PVDF powder and neat PVDF film, c) FT-IR spectrum of NBT-BT powder and d) FT-IR spectrum of flexible films.

Table 1
Amount of α (F_α), and electroactive phases, β (F_β), γ phases (F_γ) and the crystallinity degree (X_C) in all composite flexible films, calculated via infrared spectroscopy and differential scanning calorimetry (DSC).

SAMPLE	$\%F_\alpha$	$\%F_\beta$	$\%F_\gamma$	X_c
PVDF	46	4	50	50
NBT-BT-PVDF30	35	45	20	44
NBT-BT-PVDF35	50	32	18	40
NBT-BT-PVDF40	44	7	49	42

whose intensity increases by increasing the filler amount, is due to the NBT-BT, and, in particular, to the metal-oxygen (M-O) stretching vibrations. In all the composites the peaks characteristic of the two electroactive phases (i.e., β and γ) are identifiable but with a different intensity depending on the film composition. Eq. (1) was used to calculate the electroactive phase (F_{EA}, constituted of F_β and F_γ) and the α-phase amount derived by difference, which are reported in Table 1. It seems that the highest amount of electroactive phases is found in the NBT-BT/PVDF 30/70 sample 65%, of which 45% of the most desirable ferroelectric β-phase [37,45,50,54,55].

The ATR-FTIR results are in accordance with the calorimetric analysis. The DSC thermograms are reported in Fig. S4. Because the melting behavior of PVDF depends not only on the polymorphism but also on other characteristics such as crystallite size and defects, a range of melting temperatures for the different crystalline phases is reported in the literature [32]. Anyhow, the β-crystallites show a melting temperature similar to that of α-form while, when the γ phase is obtained by crystallization from the melt as in the present case, its melting peak is about 8–10 °C higher than those of the other two polymorphs.

The DSC melting curves reported in Fig. S4 show that, in the case of the hot-pressed PVDF and its composite containing 40 vol% of NBT-BT both characterized by a large amount of γ phase, beside the main peak centered at about 160 °C a shoulder is clearly visible at higher temperatures (about 170 °C).

Since Eq. (1) allows calculating the relative amount of the crystalline phases without taking into account the overall quantity of PVDF crystalline phase with respect to the amorphous counterpart, the crystallinity degrees of the samples were calculated as well. As visible from Table 1, the presence of the particles reduces the overall crystallinity degree of PVDF, but, being the X_c values comparable for all the composites, the trends observed for the different polymorphs remain valid.

Mohanty et al. [45] have shown that the negative electrostatic charge of nanoparticles of the filler is used to potentiate the nucleation of β-phase in PVDF. These authors worked on NBT-BT/PVDF films obtained by the solution casting method and pointed out that the negatively charged surface of the NBT-BT confirmed by the zeta potential measurement, enabled mostly the formation of β-phase. Actually, the CH_2 bonds of the PVDF and the negatively charged

surface of NBT-BT particles have a strong interaction, which induced extended TTTT conformation aligned on the surface of nanoparticles and resulted in the formation of the β-phase [31,37,45]. It was also demonstrated that there is possibly a critical limit of filler amount that leads to the restricted formation of β-phase. After a certain concentration of filler, particles were prone to agglomeration and thus the ionic dipole interactions are getting weaker and the number of centers for the nucleation of β-phase decrease. The results obtained in the investigated case are partially in agreement with the data obtained from Mohanty et al. Here, the presence of NBT-BT filler in the polymer matrix indeed potentiates the formation of β-phase in the films; however, the amount of β-phase decreases with filler amount probably due to differences in the methods used for the preparation of the films in compared studies [45]. Notwithstanding this, the existence of electroactive β-phase in the film will surely improve its electrical properties and broaden its possible applications.

Since NBT-BT ceramic filler and PVDF polymer are materials with significantly different properties, the electrical properties of their composites are influenced not only by the relative permittivity of the polymer and the filler, but also by other factors such as the morphology of the filler, its dispersion, volume fraction of the filler, structural defects and pores, the existence of different molecular conformations of PVDF and interactions between the obtained phases [2,45,56,57]. It is also important to note that in flexible films consisting of functional material embedded in a polymer matrix, the effective distance between the electrodes and effective electrode area can vary (due to small variations of the film thickness) and can complicate the interpretation of the electric and ferroelectric experimental data.

The temperature dependence of the dielectric permittivity, ε` and loss tangent, tan δ at different frequencies of the flexible composites and neat PVDF are presented in Fig. 3a–d. The dielectric permittivity value of each composite is lower in comparison with NBT-BT (6% BT) dielectric permittivity value, which is about 2000 [25,26] but higher than dielectric permittivity of neat PVDF film ~ 10 [7,39].

There is an effect of the increase of the active phase concentration in the film: the dielectric permittivity for 40 vol% is nearly two times higher than for 30 vol% and eight times higher than for neat PVDF, while the losses at room temperature (measured at the standard frequency of 1 kHz) remain below 3% (Fig. 3a–d). Although the dielectric permittivity around ~ 80 obtained for these samples is much smaller than that of neat NBT-BT ceramics, it is however a much higher value in comparison with similar composites reported in other works [45,46,58–60].

This is illustrated in the Table 2, where a comparison of dielectric permittivity and loss (at RT and frequency 1 kHz) from various lead-free ferroelectric ceramics/PVDF compositions is given. Results reported in the literature have been selected for those compositions with relatively low dielectric loss tangent. Higher amount of NBT-BT filler results into poorer dispersion in the polymer which is followed by the formation of more structural defects and pores in the composite. The existing literature data suggested rather different concepts regarding dielectric properties of different PVDF polymorphs in neat films. The main issue is that different processing methods can tune the polymorphism of PVDF films and change the characteristics of the polymer such as: the degree of crystallinity, the polymer chains orientation, the size of the crystals etc. In this regard, besides the effect of the amount of NBT-BT filler on dielectric properties, the type of PVDF polymorphism formed in the flexible film was also considered as important factor (see FT-IR results). W. Xia et al. who presented the study about PVDF polymers and its properties prepared by casting and further quenching, suggested that non polar α- phase possesses higher value dielectric permittivity than β-and γ-PVDF phases [37]. Similarly, S. Muduli et al. have shown in their work, in which neat PVDF films were prepared by solvent casting and later hot pressing, that an increase of β-phase fraction reduces the dielectric constant [53]. On the contrary, R. Gregorio et al. prepared melting solution casted PVDF films and noticed that in the samples with predominantly β-phase the dielectric permittivity was higher [61]. Yang et al. prepared PVDF films by solvent casting and passed them through the rolling machine in order to increase their β-phase content, pointing that films with higher amount of β-phase possessed enhanced dielectric properties [49].

In our case, sample NBT-BT/PVDF 30/70 has the lowest value of ε′, having the lowest amount of filler but also the highest concentration of β-phase among all composites. Even though the specimen NBT-BT/PVDF 40/60 possesses the lowest amount of β-phase, its dielectric permittivity value is the highest. The results show that there is an increasing trend in dielectric permittivity with β-phase fraction decrease. However, it seems that the dielectric permittivity value of all obtained composites is mostly affected by the filler amount rather than the crystalline phases formed in the films [37,57]. The dielectric permittivity values for all samples are almost frequency independent in the low temperature region (up to 200 K), but above this temperature, a region of dispersion emerges below room temperature. The most prominent dielectric dispersion can be seen for temperatures between 200 and 350 K. The main feature is the shift of the maximum of dielectric loss toward higher temperatures with the increase of the measurement frequency, which should be due to the effect of freezing of dipolar motion in the amorphous PVDF matrix. This can be noticed for the neat PVDF and all composite films as well [7]. The dielectric response of the composites in this region is mainly determined by the response of the PVDF polymer and its glass transition [7,62].

By a closer look at Fig. 3, one can also register a very useful zone around room temperature as a plateau with relatively constant dielectric permittivity and losses. The broad relaxor peak characteristic for the NBT-BT (6% BT) ceramics expected in the region between 400 and 550 K is missing from the dielectric spectrum since it is out of the measurement range [25,26,63]. Despite that, the tangent losses of all composites start curving down above 400 K which may be correlated with the dielectric relaxation caused by the NBT-BT filler. Some authors suggested that this relaxation can be attributed also to the wide oscillation angle of polymer polar groups followed by their rotation with main chain co-operation [2,7].

For anelastic measurements three strips were cut from circular films of all NBT-BT/PVDF and excited on their flexural modes. The fundamental resonance frequency is:

$$f_1 = 1{\cdot}028(t/l^2)(E/\rho)^{1/2}, \quad (2)$$

where t, l, E and ρ are the sample thickness, length, Young's modulus and density. The Young's modulus was evaluated from this formula with an error of the order of 20% due to the non-uniform thickness, especially for the 35% sample (Fig. 4a). Other sources of error are possibly non-uniform density and the metallic electrode. The elastic energy loss, or reciprocal of the mechanical quality factor, $Q^{-1} = E''/E'$, was evaluated from the width of the resonance curves. Higher frequencies were probed by exciting during the same temperature run the 3rd flexural mode, with $f_3 \cong 5.4f_1$ and higher modes when possible. Fig. 4b presents the temperature dependence of the Young's modulus and elastic energy loss of NBT-BT/PVDF 40/60 measured on three flexural modes during heating. The curves are relatively stable, and the gray line had been obtained three days before on cooling. The temperature dependence of the Young's modulus and the losses are dominated by those of the polymer, but the magnitude of the modulus is larger of a factor ~3 with respect to PVDF due to the rigid ceramic fraction, similarly to the dielectric permittivity [7].

All the three major Q^{-1} peaks and the corresponding steps in the modulus shift to higher temperature with increasing frequency and

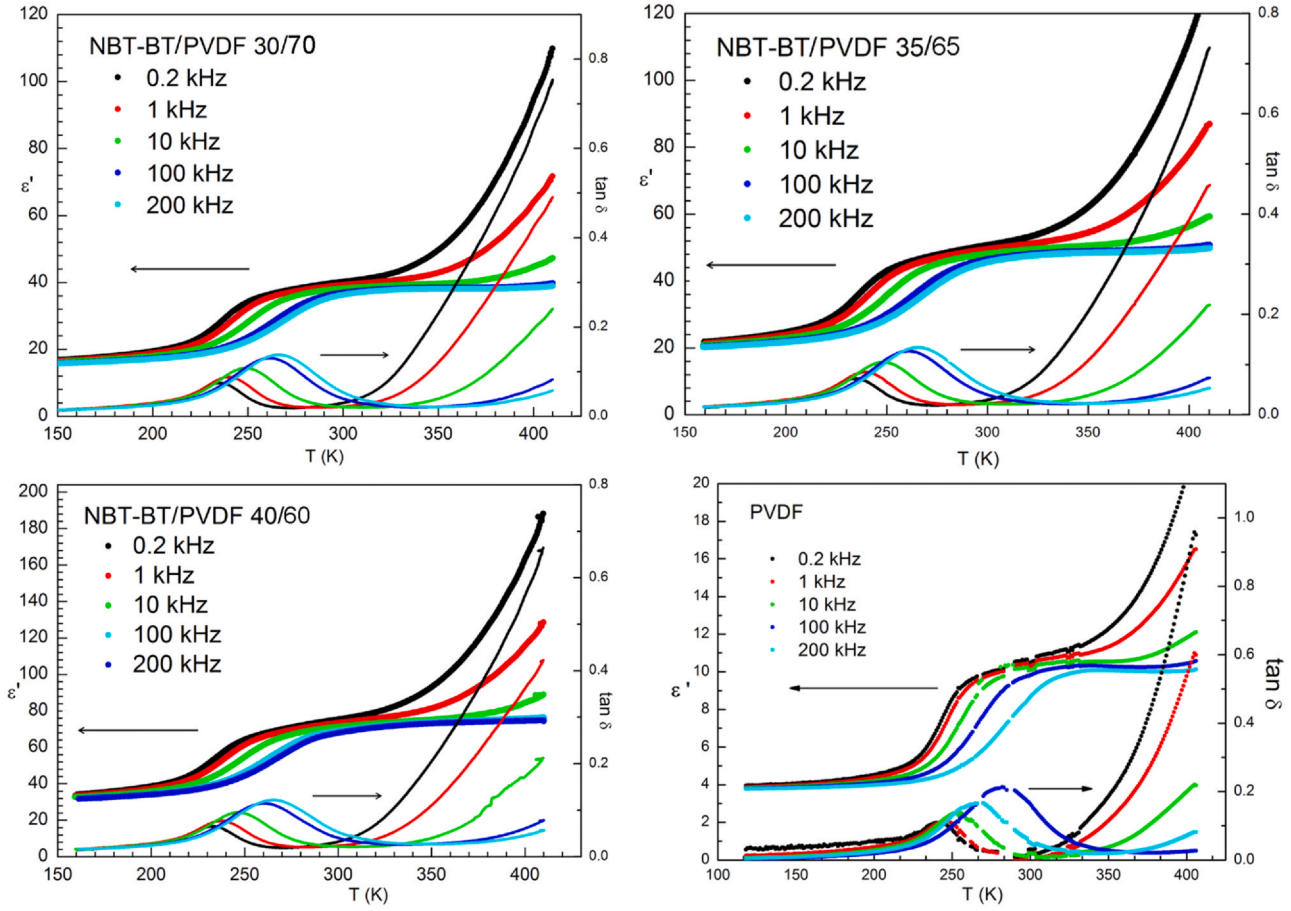

Fig. 3. Fig. 3. Dielectric permittivity and dielectric losses vs. temperature for NBT-BT/PVDF flexible films for different compositions and frequencies, as specified on the graphs: a) NBT-BT/PVDF 30–70; b) NBT-BT/PVDF 35/65; c) NBT-BT/PVDF 40/60; d) PVDF. All the curves have been measured during cooling procedure.

Table 2
Comparison of dielectric permittivity and dielectric loss tangent (at RT and f = 1 kHz) obtained in this work with those reported in the literature on other lead-free ferroelectric ceramics/PVDF flexible composites. (The values reported in this work are obtained from the corresponding curves in Fig. 3 measured on cooling at 1 kHz, by averaging the results around room temperature).

SAMPLE	Ceramic concentr. (%)	Dielectric permittivity	Dielectric loss tan ö	Ref.
NBT-BT/PVDF	30	40	0.02	This work
NBT-BT/PVDF	35	48	0.02	This work
NBT-BT/PVDF	40	78	0.03	This work
NBT-BT/PVDF	30	11	0.05	[45]
NBT-BT/PVDF	40	10	0.03	[45]
NBT-BT/PVDF	30	18	0.03	[46]
$BaTiO_3$/PVDF	40	65	0.02	[58]
$BaTiO_3$/PVDF	40	51	0.03	[59]
BCTZ/PVDF	35	22	0.025	[60]
BCTZ/PVDF	45	24.5	0.028	[60]

certainly correspond to those in the dielectric permittivity (the permittivity, ε should be compared with 1/*E*). Table 3 summarizes the density, measured with Archimedes method, the fundamental resonance frequency at room temperature and the corresponding Young's modulus of the three compositions and of a pure PVDF sample. Notice that the resonance frequency depends considerably on *T*, for example from 212 Hz to 650 Hz with cooling for the 40% sample. As expected, there is stiffening with increase of the ceramic fraction. The local minimum of *E* at 35% is within the experimental error due to the non-homogeneous thickness, but also reflects a minimum in density.

P-E hysteresis loops of pure PVDF and its composites measured at room temperature, at 170 kV/cm and frequency of 100 Hz are presented in Fig. 5a. The hysteresis loops are well defined but not saturated and therefore the remnant polarization values of the films cannot be compared with high accuracy. The saturation was not reached possibly due to the limitation of the voltage source (4000 V). This can be seen in the literature quite often for the composite films made of PVDF with other different fillers, such as, PZT, PLZT, BT, NBT etc. [2,22,57,64,65]. Many parameters can influence the ferroelectric properties such as interface areas, agglomerations, voids in the composites, inhomogeneous distribution of filler in the polymer matrix etc. [2,64,65]. However, as mentioned previously, there are a couple of more important effects that can influence the ferroelectric properties of these composite materials and have to be considered. The sintered NBT-BT ceramics possesses good ferroelectric properties with nicely saturated square shaped hysteresis loop measured at 50 kV/cm with P_r = 38 μC/cm^2 and E_c= 30 kV/cm (Fig. 5b), which is in agreement with the data available from the literature [66,67].

Likewise, the literature about ferroelectric properties of pure α, β and γ PVDF films points to the possibility of a profound effect of PVDF phases on the ferroelectric properties of the composites [36,37,45,55,57,68]. Neat β- phase PVDF shows typical characteristic of normal ferroelectric in the squared shaped loops for its all-trans conformations. α- and γ- PVDF phases have smaller remnant polarization under the same conditions, and P_r of γ-PVDF is slightly higher than that of α-PVDF which can be attributed to the T3G conformation which is more polar than TGTG` of α-PVDF [36,37].

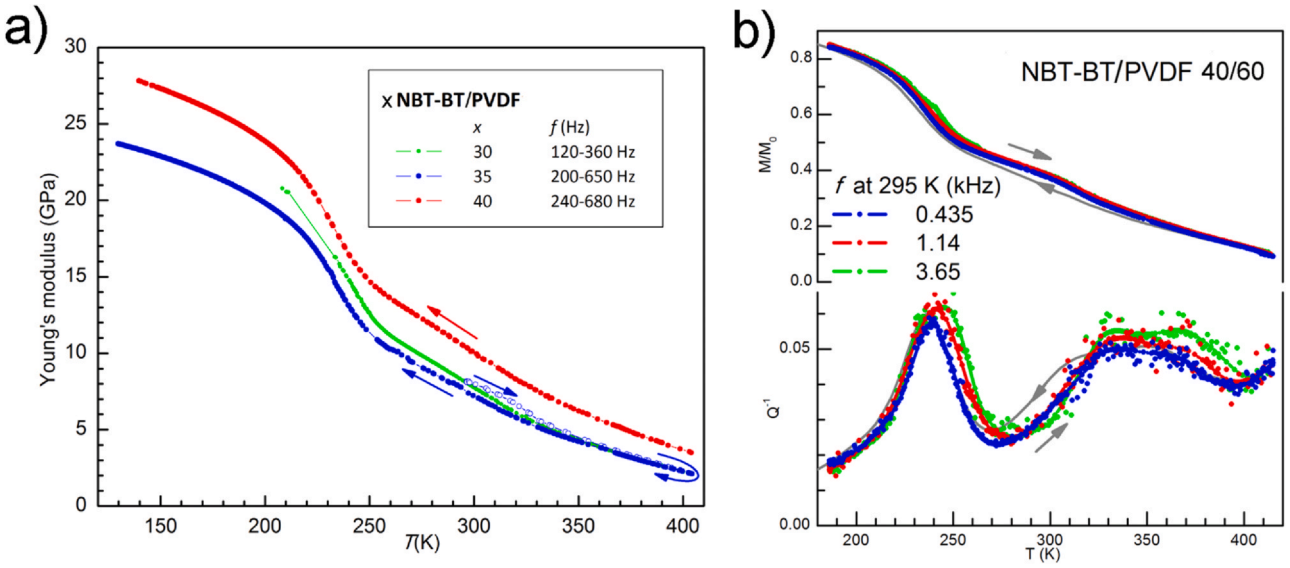

Fig. 4. a) Young's modulus measured exciting the 1st flexural mode of a pure PVDF and NBT-BT/PVDF 30/70, 35/65 and 40/60 composite samples during cooling; the initial heating is also shown for the 35% sample (empty symbols) and b) Relative change of the Young's modulus and elastic energy loss vs. *T* of NBT-BT/PVDF 40/60 measured alternately exciting three flexural resonances during a same heating run.

Table 3
The density, measured with Archimedes's method, the fundamental resonance frequency at room temperature and the corresponding Young's modulus of the three compositions.

x	ρ (g/cm^3)	f_1 (Hz) at 295 K	*E* (GPa) at 295 K
0	1.7	960	2.1 ± 0.2
30	3.06 ± 0.066	230	8.1 ± 0.8
35	2.95 ± 0.06	370	7.6 ± 1.3
40	3.32 ± 0.06	420	10.5 ± 1

Thus, as it can be noticed from Fig. 5a, in our case there is a combined effect of both, influence of the filler amount and effect of PVDF crystal phases present in each film. The NBT-BT/PVDF 30/70 has the lowest amount of the filler but also the highest concentration of the ferroelectric β- phase, 45% and it shows a bit lower P_r and E_c values in comparison with the NBT-BT/PVDF 35/65 sample that has 32% of β- phase but a higher concentration of the filler.

The largest loop area which is connected with high losses can be seen for the NBT-BT/PVDF 40/60 sample that possesses the highest amount of filler but the lowest concentration of the ferroelectric β- phase ~7%.

In order to confirm that the polarization arises due to intrinsic dipoles, room-temperature pulsed polarization positive up-negative down (PUND) measurements of composites have been carried out with delay time of 0.2 ms and pulse weight 0.1 ms at 170 kV/cm. Detailed explanation of PUND method and obtained results are presented in Fig. S5 and Supplementary material [69–71]. From the presented results, it can be concluded that samples with higher concentration of filler indeed have higher value of remnant polarization. In order to give a clearer picture more detailed study have to be performed for the future study.

3.3. Application point of view: Energy storage and Energy harvesting

3.3.1. Energy storage

During the recent years researchers have been studying PVDF based composites reinforced with various fillers, e.g., PZT, BT, BST, TiO_2 etc. for developing energy storage materials [50,57,65,72,73]. Here, regarding the resulting dielectric and ferroeletric properties of the flexible composites obtained in this study, the potential of these materials for the energy storage application was investigated. High values of breakdown strength and dielectric permittivity are defined as two main factors that can determine energy storage potential of the material [57].

As it was presented, the NBT-BT ceramic filler exhibits much higher values of dielectric permittivity in comparison with PVDF polymer. On the other hand, the breakdown strength signifies the highest electric field applicable to the dielectric materials. In this study, due to the limitation of the used instrumentation, the electric breakdown strengths values for each composite was not reached, but from the E_{max} presented in the Table 4 it can be assumed that the amount of filler affects the properties necessary for the energy storage application. As the amount of the filler increases, more inhomogeneous distribution of the filler in the polymer occurs; more voids and defects are formed, causing the local electric field concentration increase and contemporary reduction of the breakdown strength of the composite materials in comparison with neat PVDF [45,56,57,74].

Typical electric displacement-electric field loops at moderate applied field of 170 kV/cm for all investigated films, are presented in the Fig. 5c. Derived values for energy density presented in the Table 4 show that the energy density became higher with the amount of NBT-BT filler in the polymer matrix and for the sample NBT-BT/PVDF 40/60 it reaches the value of 0.148 J/cm^3. The energy density is getting higher with the increase of electric field as well, e.g. in the sample NBT-BT/PVDF 35/65 it changes from 0.108 J/cm^3 at 170 kV/cm to 0.172 J/cm^3 at 210 kV/cm. Literature data have shown that similar PVDF based composite films (with different fillers: pure and doped barium titanate, strontium titanate, barium strontium titanate, etc.) possess energy density in the range 2–7 J/cm^3 measured at 1000–4000 kV/cm [57,75]. However, due to limitation of our equipment, much lower fields were reached and therefore the values obtained for energy density are accordingly lower. Thus, it is difficult to compare the results obtained from the present study and results available in the literature since the measurements were performed in different conditions. The obtained results can nevertheless point on the materials potential for this application. Besides high energy density, for the practical application in the energy storage devices, it is important that the material possesses great efficiency. Energy density efficiencies obtained from the D-E loops for investigated materials are presented in the Table 4, showing a decreasing trend with increasing amount of NBT-BT (from 74 down to 66%). Lower

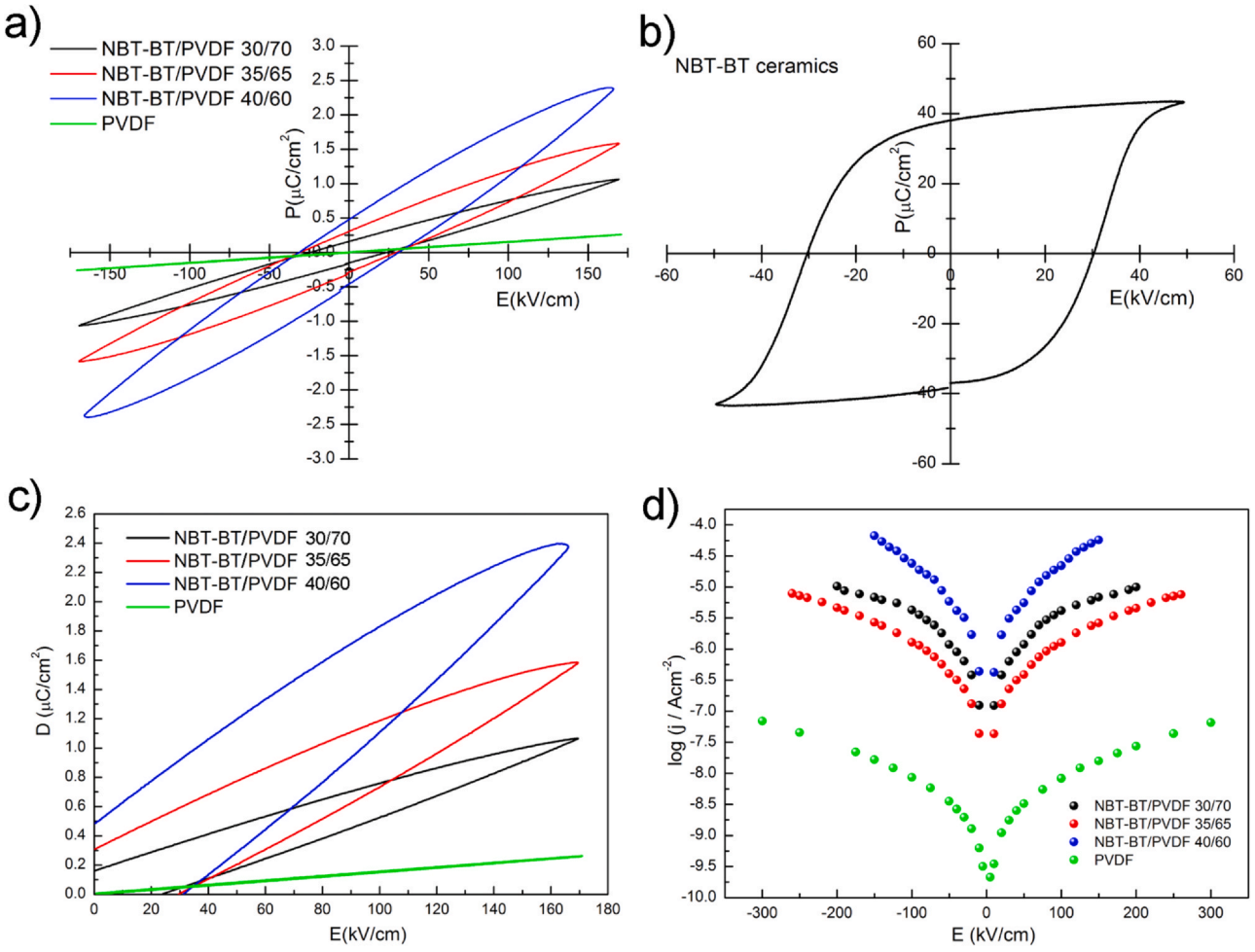

Fig. 5. Ferroelectric properties of neat PVDF and all composite films at a) 170 kV/cm, b) hysteresis loop of NBT-BT ceramics, c) Displacement vs. electric field loops and d) leakage current density vs. electric field for neat PVDF and all composite flexible films.

values of efficiency in comparison with pure PVDF (94%), may be probably attributed to the larger leakage current in the composite films [45,50,57].

Low leakage current density is also an important parameter for the application of the material for energy storage. Leakage current density (j) was measured as a function of static electric-field (E) in order to study the conductivity in the material and it is presented in Fig. 5d. Keeping in mind that the leakage current is related to the electric conductivity, the obtained results imply the highest electrical conductivity of the NBT-BT/PVDF 40/60 which is followed by slight decrease for the samples NBT-BT/PVDF 30/70 and NBT-BT/PVDF 35/65, respectively. Significantly lower leakage current density was measured for neat PVDF flexible film. Since both component phases, PVDF and NBT-BT, show low conductivity, it means that the conductive channels are created in the composite phase. Indeed, as it was suggested earlier, the amount of ceramic filler can cause the formation of more defects, pores and space charge in the composite, and worsen the mechanical properties and flexibility, provoking the increase of the leakage current density and affecting the energy storage properties as well [2,23,68,74]. Detailed analysis of leakage current mechanisms pointed on possible existence of both, ohmic and space charge limited conduction in all investigated films. With the filler amount increase, the conduction is more likely to be due to space charge limited conduction, especially in the higher field region [76–78]. Details can be found in the Supplementary material (Fig. S6).

According to all the data available, nanoparticles such as the ones used in this study, were found to have strong mutual interaction and cause the agglomeration of the filler and its non uniform distribution in the films that influence energy storage properties [57,75,79]. In order to improve the energy storage density, two future aspects will be examined. The first one will be the modification of nanoparticles by the hydroxylation process in which the interaction of the filler nanoparticles with PVDF are stronger and its compatibility becomes better which can improve the breakdown strength of the composite. Y. Wang et al. indicated that using hydroxylated barium titanate nanoparticles instead of as prepared ones, increased the energy storage density up to 3.7 J/cm^3. On the other hand, using the fillers

Table 4
Electric displacement, maximum electric field, dielectric permittivity values at 1 kHz, energy storage density and energy density efficiency for composites and neat PVDF film.

Sample	D (μC/cm^2)	E_{max} (kV/cm)	ε_r (at 1 kHz)	J (J/cm^3)	η (%)
PVDF	0.23	400	11	0.017	96.60
NBT-BT/PVDF 30/70	1.06	330	40	0.0765	74.38
NBT-BT/PVDF 35/65	1.58	260	50	0.108	68.35
NBT-BT/PVDF 40/60	2.30	150	73	0.148	66.37

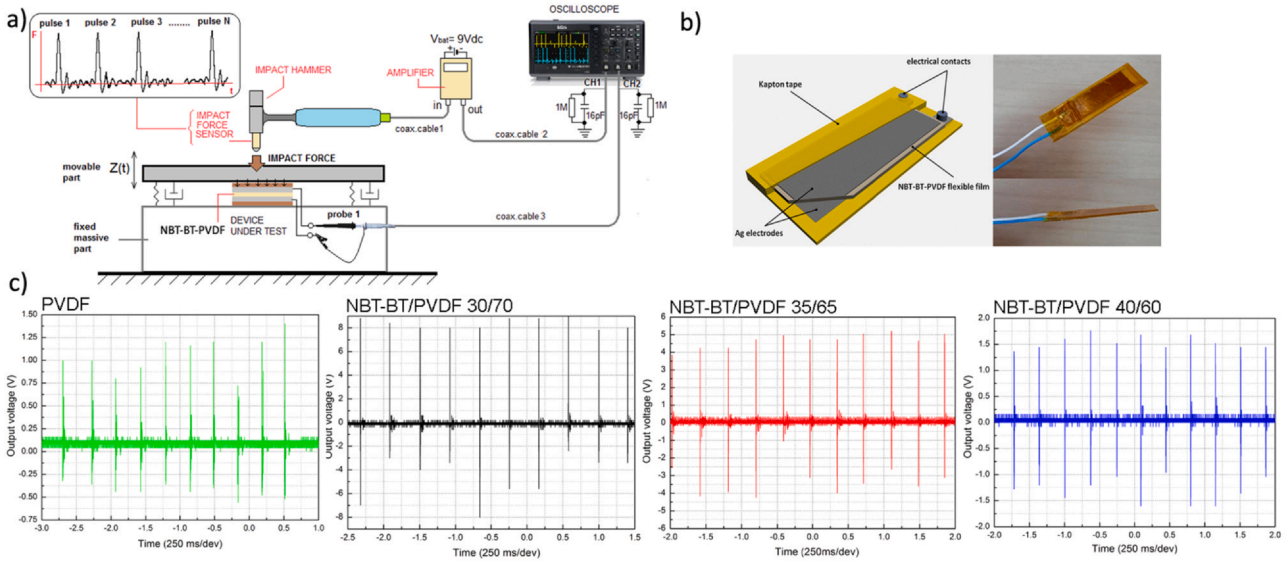

Fig. 6. a) Scheme of testing set-up and b) Scheme of the energy harvesting and storage component and picture of the assembled one, c) Oscilloscopic records of the voltage output obtained by applying the impact force.

with a larger aspect ratio nanofibers, nanotubes or nanosheets can induce better energy storage performance [57,75,79].

3.3.2. Energy harvesting

Piezoelectric polymers typically provide lower power output in the micro Watt range, smaller in comparison with the piezo-ceramic energy harvester based on PZT [80]. In order to combine good piezoelectric properties of the ceramics and flexibility of the polymers, composites consisting of ceramic filler incorporated in the polymer matrix are being developed extensively during the last decade [4,27,80,81].

In this study, poled lead-free flexible films were electroded with silver and wired with Cu wires in order to enable the connection with external circuit. The energy harvester unit was encapsulated in the two layers of thin Kapton tape which is a protective layer and gives dimensional stability to the device (see Fig. 6b).

In order to achieve uniform distribution of mechanical stress on the sample, the sample was placed in the holder between sandwich like metal plates with two springs at the ends of the bottom plate. Thus, after each mechanical impact of impulse hammer, springs were able to return the upper metal plate into the original position. The scheme of the testing set-up with all used mechanical and measuring equipment was presented in Fig. 6a.

Voltage generation of polymer/ceramic composites NBT-BT/PVDF while applying the impact force of 250 N are presented in Fig. 6c. The highest value of the output voltage was 8–9 V for NBT-BT/PVDF 30/70, 4–5 V for NBT-BT/PVDF 35/65 and around 1.5 V for NBT-BT/PVDF 40–60. The highest values of output current ~ 8–9 μA and maximum of generated power up to 80 μW were obtained for the NBT-BT/PVDF 30–70 (Fig. S7). Accordingly, lower values were achieved for other two samples and the lowest voltage output was found in the neat PVDF flexible films ~ 1 V.

The explanations for the voltage output decrease with filler amount increase can be the agglomeration of filler particles and non-completely homogeneous distribution of the filler in the polymer matrix, supported by the literature data [22,45,74,80] and proven by measured density values of the composites. On the other hand, another possible explanation could be found in PVDF polymorphism. According to the literature data, with the poling method used in this study, in which PVDF films were under the influence of high field and high temperature for almost 1.5 h, polymorphic changes of PVDF are expected [32,37,45,50]. The issue of polymorphism changes could be probably solved by the corona poling method, in which PVDF samples are exposed to extreme poling conditions for a short period of time, which is not enough for significant changes in the polymer structure [82–84]. Nevertheless, this investigation will be, conducted as a topic of the some future study.

According to the above, these enhanced properties in the NBT-BT/PVDF 30/70 can be probably attributed to better distribution of the filler in this flexible composite and higher amount of electroactive phases.

Additionally, the piezoelectric charge constants, d_{33}, were determined using the equation: d_{33}= -C*V/F, where C is the capacitance of the film (pF), V is the output voltage (V) and F is the applied force (N) [82,83]. The values obtained were 16; 7 and 2 pC/N for NBT-BT/PVDF samples, with the amount of filler, respectively and 2 pC/N for neat PVDF film. The results are in accordance with the measured output voltage values.

For a closer comparison, the power consumption of a typical solar-powered calculator, is about 5 microwatts and that of a typical digital thermometer with a liquid crystal display is only one microwatt. As it was shown, this kind of harvester (1.5 cm^2) can collect enough power to produce about 80 microwatts of DC power that is enough for many sensing (humidity, temperature sensors) and computing jobs.

4. Conclusion

Flexible polymer/ceramics composite films were successfully prepared by adding lead-free piezoelectric material sodium bismuth titanate-barium titanate (NBT-BT) into a polymer polyvinylidene fluoride (PVDF) matrix by hot pressing. Flexible films with different filler amount were prepared and investigated. Detailed structural analysis of films leads to the conclusions that the hot pressing method partially induced the formation of electroactive β-phase of PVDF polymer, influencing in that way the electrical properties of the material. Even NBT-BT as filler with negatively charged surface can favor a predominant formation of desirable piezoelectric PVDF phase. The dielectric permittivity of the films obtained in this study was much higher in comparison with the one obtained from other authors. NBT-BT/PVDF 40/60 had nearly two times higher values of dielectric permittivity than NBT-BT/PVDF 30/70 and eight times higher than neat PVDF, while the losses at room temperature

(measured at the standard frequency 1 kHz) remained below 3%. A very useful zone around room temperature as a plateau with relatively constant dielectric permittivity and losses was noticed in the dielectric spectra of each film. Anelastic measurements showed a complete agreement with dielectric properties in which the temperature dependence of the Young's modulus and the losses are dominated by those of the polymer, but the magnitude of the modulus is larger of a factor ~3 with respect to PVDF due to the rigid ceramic fraction. Non-saturated hysteresis loops pointed out the combined effect of two factors, that is influence of the filler amount and effect of PVDF crystal phases present in each film. Calculations of energy storage density and energy density efficiencies obtained for the investigated materials revealed a decreasing trend with increasing amount of NBT-BT. The values of $\eta = 66–74\%$ that were obtained for all the composites, were determined as high enough for the practical application of these materials.

Assembled energy harvesting units were made by proper wiring and covering the flexible film with a Kapton protection layer. Charge generation of polymer/ceramics composites while applying the impact force was investigated. The highest value of the output voltage was 9 V and it was obtained for NBT-BT/PVDF 30/70 (4.5 V for NBT-BT/PVDF 35/65 and 1.5 V for NBT-BT/PVDF 40/60). The highest values of output current was ~ 9 μA and maximum of generated power was up to 80 μW.

The main conclusion derived from this study is that flexible composite films made of lead-free NBT-BT filler and PVDF matrix, especially NBT-BT/PVDF 30/70, have high potential to be used for efficient environmentally safe low-energy storage and harvesting devices.

CRediT authorship contribution statement

Mirjana Vijatovic Petrovic: Conceptualization, Writing - original draft, Writing - review and editing, Methodology, Investigation, Data analysis, Project administration, Supervision. **Francesco Cordero:** Investigation, Data analysis, Writing - review & editing. **Elisa Mercadelli:** Methodology, Writing - review & editing. **Nikola Ilic:** Investigation, Methodology, Data analysis. **Elisabetta Brunengo:** Investigation, Formal analysis, Writing - Review & Editing. **Carmen Galassi:** Conceptualization, Writing: review & editing. **Zeljko Despotovic:** Methodology, Data analysis, Data curation. **Jelena Bobic:** Methodology, Data analysis, Formal analysis. **Adis Dzunuzovic:** Methodology, Data curation. **Paola Stagnaro:** Conceptualization, Resources, Writing - Review & Editing. **Giovanna Canu:** Methodology, Writing - review & editing. **Floriana Craciun:** Investigation, Data analysis, Writing - review & editing, Project administration, Supervision.

Declaration of Competing Interest

The authors declare that they have no known competing financial interests or personal relationships that could have appeared to influence the work reported in this paper.

Acknowledgements

The authors gratefully acknowledge the Ministry of Education, Science and Technological Development Republic of Serbia to financial support given through national programs (project code 451-03-68/2020-14/200053) and bilateral project (project code in SR 451-03-03064/2018-09/1) "Lead-free piezoelectric and multiferroic flexible films for nanoelectronics and energy harvesting" with Italy and Ministry of Foreign Affairs and International Cooperation of Italy (project code: RS19MO01). Claudio Capiani from CNR-ISTEC for the preparation of the NBT-BT powders and dr Maria Teresa Buscaglia from CNR-ICMATE for SEM analysis of NBT-BT powder are gratefully acknowledged.

Appendix A. Supporting information

Supplementary data associated with this article can be found in the online version at doi:10.1016/j.jallcom.2021.161071.

References

[1] Y. Lua, J. Chena, Z. Chenga, S. Zhanga, The PZT/Ni unimorph magnetoelectric energy harvester for wireless sensing applications, Energy Convers. Manag. 200 (2019) 112084.
[2] J.D. Bobic, G. Ferreira Teixeira, R. Grigalaitis, S. Gyergyek, M.M. Vijatović Petrovic, M. Ap Zaghete, B.D. Stojanovic, PZT–NZF/CF ferrite flexible thick films: structural, dielectric, ferroelectric, and magnetic characterization, J. Adv. Ceram. 8 (4) (2019) 545–554.
[3] A.K. Sharma, J.K. Swamy, A. Jain, Dielectric properties of PVDF-PZT composite films and their thermal dependence, Adv. Mater. Proc. 1 (2) (2016) 185–190.
[4] S.H. Wankhade, S. Tiwari, A. Gaur, P. Maiti, PVDF–PZT nanohybrid based nanogenerator for energy harvesting applications, Energy Rep. 6 (2020) 358–364.
[5] S.K. Sharma, H. Gaur, M. Kulkarni, G. Patil, B. Bhattacharya, A. Sharma, PZT–PDMS composite for active damping of vibrations, Compos. Sci. Technol. 77 (2013) 42–51.
[6] D.P. Anh, D.V. On, D.A. Quang, N. Van Thinh, N.T. Anh Tuyet, V. Thanh Tung, T. Van, Chuong, dielectric and piezoelectric properties of PZT/PVDF composites prepared by hot press method, Inter. J. Eng. Res. Technol. 9 (4) (2020) 898–902.
[7] B. Hilczer, J. Kułek, E. Markiewicz, M. Kosec, B. Malic, Dielectric relaxation in ferroelectric PZT–PVDF nanocomposites, J. Non-Cryst. Solids 305 (2002) 167–173.
[8] B. Li, Q. Liu, X. Tang, T. Zhang, Y. Jiang, W. Li, J. Luo, High energy storage density and impedance response of PLZT2/95/5 antiferroelectric ceramics, Materials 10 (2017) 143.
[9] A. Jain, K.J. Prashanth, A. Kr Sharma, A. Jain, P.N. Rashmi, Dielectric and piezoelectric properties of PVDF/PZT composites: a review, Polym. Eng. Sci. 55 (7) (2015) 1589–1616.
[10] N. Cai, J. Zhai, C.-W. Nan, Y. Lin, Z. Shi, Dielectric, ferroelectric, magnetic, and magnetoelectric properties of multiferroic laminated composites, Phys. Rev. B 68 (2003) 224103.
[11] T. Siponkoski, M. Nelo, J. Palosaari, J. Perantie, M. Sobocinski, J. Juuti, H. Jantunen, Electromechanical properties of PZT/P(VDF-TrFE) composite ink printed on a flexible organic substrate, Compos. Part B 80 (2015) 217–222.
[12] J. Rödel, K.G. Webber, R. Dittmer, W. Job, M. Kimurac, D. Damjanovic, Transferring lead-free piezoelectric ceramics into application, J. Eur. Ceram. Soc. 35 (2015) 1659–1681.
[13] H. Zhang, W. Ma, B. Xie, L. Zhang, S. Dong, P. Fan, K. Wang, J. Koruza, J. Rodel, Na1/2Bi1/2)TiO3–based lead-free co-fired multilayer actuators with large strain and high fatigue resistance, J. Am. Ceram. Soc. 102 (2019) 6147–6155.
[14] M.I. Bichurin, D.A. Filippov, V.M. Petrov, V.M. Laletsin, N. Paddubnaya, G. Srinivasan, Resonance magnetoelectric effects in layered magnetostrictive-piezoelectric composites, Phys. Rev. B 68 (2003) 132408.
[15] J.I. Roscow, Y. Zhang, M.J. Kraśny, R.W.C. Lewis, J. Taylor, C.R. Bowen, Freeze cast porous barium titanate for enhanced piezoelectric energy harvesting, J. Phys. D: Appl. Phys. 51 (2018) 225301.
[16] L.-Feng Zhu, B.-Ping Zhang, L. Zhaoa, J.-Feng Lib, High piezoelectricity of BaTiO3–CaTiO3–BaSnO3 lead-free ceramics, J. Mater. Chem. C. 2 (2014) 4764–4771.
[17] M. Cernea, L. Trupina, B.S. Vasile, R. Trusca, C. Chirila, Nanotubes of piezoelectric BNT–BT0.08 obtained from sol–gel precursor, J. Nanopart. Res. 15 (2013) 1787.
[18] S.-Tao Zhang, A. Brice Kounga, E. Aulbach, T. Granzow, W. Jo, H.-Joachim Kleebe, J. Rödel, Lead-free piezoceramics with giant strain in the system Bi 0.5Na0.5TiO3 – BaTiO3– K0.5Na0.5NbO3 I. Structure and room temperature properties, J. Appl. Phys. 103 (2008) 034107.
[19] W. Liu, X. Ren, Large piezoelectric effect in pb-free ceramics, Phys. Rev. Lett. 103 (2009) 257602.
[20] Y. Liu, Y. Chang, F. Li, B. Yang, Y. Sun, J. Wu, S. Zhang, R. Wang, W. Cao, Exceptionally high piezoelectric coefficient and low strain hysteresis in grain-oriented (Ba,Ca)(Ti,Zr)O3 through integrating crystallographic texture and domain engineering, ACS Appl. Mater. Interfaces 9 (2017) 29863–29871, https://doi.org/10.1021/acsami.7b08160
[21] Z. Wang, J. Wang, X. Chao, L. Wei, B. Yang, D. Wang, Z. Yang, Synthesis, structure, dielectric, piezoelectric, and energy storage performance of (Ba0.85Ca0.15)(Ti0.9Zr0.1)O3 ceramics prepared by different methods, J. Mater. Sci. Mater. Electron. 27 (2016) 5047–5058.
[22] S. Moharana, S. Sai, R. Naresh Mahaling, Enhanced dielectric and ferroelectric properties of surface hydroxylated Na0.5Bi0.5TiO3 (NBT)-poly(vinylidene fluoride) (PVDF) composites, J. Adv. Dielectr. 08 (3) (2018) 1850017.
[23] D. Mauryaa, M. Peddigarid, M.-Gyu Kang, L.D. Geng, N. Sharpes, V. Annapureddy, H. Palneedi, R. Sriramdas, Y. Yan, H.-Cheol Song, Y.U. Wang, J. Ryub, S. Priyac, Lead-free piezoelectric materials and composites for high power density energy harvesting, J. Mat. Res. 33 (16) (2018) 2235–2263.
[24] V. Dorcet, G. Troillard, P. Boullay, Reinvestigation of phase transitions in Na0.5Bi0.5TiO3 by TEM. Part I: first order rhombohedral to orthorhombic phase transition, Chem. Mater. 20 (2008) 5061–5073.
[25] F. Cordero, F. Craciun, F. Trequattrini, E. Mercadelli, C. Galassi, Phase transitions and phase diagram of the ferroelectric perovskite (Na0.5Bi0.5)1−xBaxTiO3 by anelastic and dielectric measurements, Phys. Rev. B 81 (2010) 144124.

[26] F. Craciun, C. Galassi, R. Birjega, Electric-field-induced and spontaneous relaxor-ferroelectric phase transitions in (Na1/2Bi1/2)1 − xBaxTiO3, J. Appl. Phys. 112 (2012) 124106.
[27] F. Ru Fan, W. Tang, Z. Lin Wang, Flexible nanogenerators for energy harvesting and self-powered electronics, Adv. Mater. 28 (2016) 4283–4305.
[28] B.D. Stojanovic, A.S. Dzunuzovic, N.I. Ilic, M.M. Vijatovic Petrovic, Complex composites: polymer matrix-ferroics or multiferroics, in: B.D. Stojanovic, G. Korotcenkov (Eds.), Magnetic, Ferroelectric, and Multiferroic Metal Oxides, Elsevier, Amsterdam, 2018, pp. 559–569.
[29] L. Mateu, T. Dra˘ger, I. Mayordomo, M. Pollak, Energy harvesting at the human body, in: E. Sazonov (Ed.), Wearable Sensors, Elsevier, Amsterdam, 2014(p).
[30] D. Lolla, M. Lolla, A. Abutaleb, H.U. Shin, D.H. Reneker, G.G. Chase, Fabrication, polarization of electrospun polyvinylidene fluoride electret fibers and effect on capturing nanoscale solid aerosols, Materials 9 (2016) 671.
[31] L. Ruan, X. Yao, Y. Chang, L. Zhou, G. Qin, X. Zhang, Properties and applications of the β Phase poly(vinylidene fluoride), Polymers 10 (2018) 228.
[32] P. Martins, A.C. Lopes, S. Lanceros-Mendez, Electroactive phases of poly(vinylidene fluoride): determination, processing and applications, Prog. Polym. Sci. 39 (2014) 683–706.
[33] A.V. Reddy, K.C. Sekhar, N. Dabra, A. Nautiyal, J.S. Hundal, N.P. Pathak, R. Nath, Ferroelectric and Magnetic Properties of Hot-pressed BiFeO3-PVDF Composite Films, International Scholarly Research Network ISRN Materials Science, 2011.
[34] A. Seema, K.R. Dayas, J.M. Varghese, PVDF-PZT-5H composites prepared by hot press and tape casting techniques, J. Appl. Polym. Sci. 106 (2007) 146–151.
[35] P. Hana, S. Panga, J. Fanb, X. Shena, T. Pan, Highly enhanced piezoelectric properties of PLZT/PVDF composite bytailoring the ceramic Curie temperature, particle size and volume fraction, Sens. Actuators A 204 (2013) 74–78.
[36] PyzoFex , PVDF and its copolymers, JOANNEUM RESEARCH, Institute for Surface Technologies and Photonics, https://www.pyzoflex.com/downloads.
[37] W. Xia, Z. Zhang, PVDF-based dielectric polymers and their application in electronic materials, IET Nanodielectr. Rev. 1 (2018) 17–31.
[38] F. Khan, T. Kowalchik, S. Roundy, R. Warren, Stretching-induced phase transitions in barium titanate-poly(vinylidene fluoride) flexible composite piezoelectric films, Scr. Mater. 193 (2021) 64–70.
[39] E. Brunengo, G. Luciano, G. Canu, M. Canetti, L. Conzatti, M. Castellano, P. Stagnaro, Double-step moulding: an effective method to induce the formation of β-phase in PVDF, Polymer 193 (2020) 122345.
[40] E. Brunengo, M. Castellano, L. Conzatti, G. Canu, V. Buscaglia, P. Stagnaro, PVDF-based composites containing PZT particles: how processing affects the final properties, J. Appl. Polym. Sci. 137 (2020) 48871.
[41] E. Brunengo, L. Conzatti, I. Schizzi, M.T. Buscaglia, G. Canu, L. Curecheriu, C. Costa, M. Castellano, L. Mitoseriu, P. Stagnaro, V. Buscaglia, Improved dielectric properties of poly(vinylidene fluoride)–BaTiO3 composites by solvent-free processing, J. Appl. Polym. Sci. 138 (2021) 50049.
[42] G.T. Davis, J.E. McKinney, M.G. Broadhurst, S.C. Roth, Electric-field-induced phase changes in poly(vinylidene fluoride), J. Appl. Phys. 49 (1978) 4998–5002.
[43] W. Kim, M. Han, Y.-H. Shin, H. Kim, First-principles study of the α-β phase transition of ferroelectric poly(vinylidene difluoride): observation of multiple transition pathways, J. Phys. Chem. B 120 (2016) 3240–3249.
[44] B. Chu, X. Zhou, K. Ren, B. Neese, M. Lin, Q. Wang, F. Bauer, Q.M. Zhang, A dielectric polymer with high electric energy density and fast discharge speed, Science 313 (2006) 334–336.
[45] H.S. Mohanty, Ravikant, A. Kumar, P.K. Kulriya, R. Thomas, D.K. Pradhan, Dielectric/ferroelectric properties of ferroelectric ceramic dispersed poly(vinylidene fluoride) with enhanced β-phase formation, Mater. Chem. Phys. 230 (2019) 221–230.
[46] S. Hajra, S. Sahoo, R.N.P. Choudhary, Fabrication and electrical characterization of (Bi0.49Na0.49Ba0.02) TiO3-PVDF thin film composites, J. Polym. Res. 26 (14) (2019) 1–11.
[47] E. Mercadelli, A. Sanson, C. Capiani, A.L. Costa, C. Galassi, Influence of the synthesis route on the properties of BNBT ceramics, Process. Appl. Ceram. 3 (2009) 73–78.
[48] H.-J. Ye, L. Yang, W.-Z. Shao, S.-B. Sun, L. Zhen, Effect of electroactive phase transformation on electron structure and dielectric properties of uniaxial stretching poly(vinylidene fluoride) films, RSC Adv. 3 (2013) 23730–23736.
[49] L. Yang, J. Qiu, K. Zhu, H. Ji, Q. Zhao, M. Shen, S. Zeng, Effect of rolling temperature on the microstructure and electric properties of β-polyvinylidene fluoride films, J. Mater. Sci. Mater. Electron. 29 (2018) 15957–15965.
[50] X. Cai, T. Lei, D. Sun, L. Lin, A critical analysis of the α, β and γ phases in poly (vinylidene fluoride) using FTIR, RSC Adv. 7 (2017) 15382–15389.
[51] A.S. Nowick, B.S. Berry Anelastic Relaxation in Crystalline Solids Academic Press, New York, 1972.
[52] F. Cordero, L. Dalla Bella, F. Corvasce, P.M. Latino, A. Morbidini, An insert for anelastic spectroscopy measurements from 80 K to 1100 K, Meas. Sci. Technol. 20 (2009) 015702.
[53] S.P. Muduli, S. Parida, S.K. Rout, S. Rajput, M. Kar, Effect of hot press temperature on β-phase, dielectric and ferroelectric properties of solvent casted poly(vinyledene fluoride) films, Mater. Res. Express 6 (2019) 095306.
[54] M. Bohle´n, K. Bolton, Conformational studies of poly(vinylidenefluoride), poly (trifluoroethylene) and poly(vinylidene fluoride-co-trifluoroethylene) using density functional theory, Phys. Chem. Chem. Phys. 16 (2014) 12929.
[55] N. Meng, X. Zhu, R. Mao, M.J. Reece, E. Bilotti, Nanoscale interfacial electroactivity in PVDF/PVDF-TrFE blended films with enhanced dielectric and ferroelectric properties, J. Mater. Chem. C 5 (2017) 3296–3305.
[56] A. Jain, K.J. Prashanth, A.K. Sharma, Dielectric and piezoelectric properties of PVDF/PZT composites: a review, Polym. Eng. Sci. 55 (2015) 1589–1616.
[57] Y. Wang, M. Yao, R. Ma, Q. Yuan, D. Yang, B. Cui, C. Ma, M. Liu, D. Hu, Design strategy of barium titanate/polyvinylidene fluoride-based nanocomposite films for high energy storage, J. Mater. Chem. A 8 (2020) 884–917.
[58] J. Fu, Y. Hou, M. Zheng, Q. Wei, M. Zhu, H. Yan, Improving dielectric properties of pvdf composites by employing surface modified strong polarized BaTiO3 particles derived by molten salt method, ACS Appl. Mater. Interfaces 7 (2015) 24480–24491.
[59] Z.M. Dang, H.Y. Wang, B. Peng, C.W. Nan, Effect of BaTiO3 size on dielectric property of BaTiO3/PVDF composites, J. Electroceram. 21 (2008) 381–384.
[60] S.A. Riquelme, K. Ramam, Dielectric and piezoelectric properties of lead free BZT-BCT/PVDF flexible composites for electronic applications, Mater. Res. Express 6 (11633) (2019) 1–11.
[61] R. Gregorio, E.M. Ueno, Effect of crystalline phase, orientation and temperature on the dielectric properties of poly(vinylidene fluoride) (PVDF), J. Mater. Sci. 34 (1999) 4489–4500.
[62] J. Banys, R. Grigalaitis, A. Mikonis, J. Macutkevic, P. Keburis, Distribution of relaxation times of relaxors: comparison with dipolar glasses, Phys. Status Solidi C 6 (12) (2009) 2725–2730.
[63] F. Cordero, F. Trequattrini, F. Craciun, E. Mercadelli, C. Galassi, Elastic and dielectric measurements of the structural transformations in the ferroelectric perovskite (Na1/2Bi1/2)1-xBaxTiO3, Solid State Phenom. 172–174 (2011) 161–165.
[64] W. Ji, H. Deng, C. Guo, C. Sun, X. Guo, F. Chen, Q. Fu, The effect of filler morphology on the dielectric performance of polyvinylidene fluoride (PVDF) based composites, Compos. Part A-Appl. S. 118 (2019) 336–343.
[65] W. Nian, Z. Wang, T. Wang, Y. Xiao, H. Chen, Significantly enhanced breakdown strength and energy density in sandwich-structured NBT/PVDF composites with strong interface barrier effect, Ceram. Int. 44 (2018) S50–S53.
[66] O. Turki, A. Slimani, L. Seveyrat, G. Sebald, V. Perrin, Z. Sassi, H. Khemakhem, L. Lebrun, Structural, dielectric, ferroelectric, and electrocaloric properties of 2% Gd2O3 doping (Na0.5Bi0.5)0.94Ba0.06TiO3 ceramics, J. Appl. Phys. 120 (2016) 054102.
[67] M. Chena, Q. Xub, B. Hee Kima, B. Kuk Ahna, J. Hoon Ko, W. Jin Kang, O. Jeong Nam, Structure and electrical properties of (Na0.5Bi0.5)1−xBaxTiO3 piezoelectric ceramics, J. Eur. Ceram. Soc. 28 (2008) 843–849.
[68] H. Luo, D. Zhang, C. Jiang, X. Yuan, C. Chen, K. Zhou, Improved dielectric properties and energy storage density of oily(vinylidene fluoride-co-hexafluoropropylene) nanocomposite with Hydration epoxy resin coated BaTiO3, ACS Appl. Meter Inter. 7 (2015) 8061–8069.
[69] P. Pal, K. Rudrapal, S. Mahana, S. Yadav, T. Paramanik, S. Mishra, K. Singh, G. Sheet, D. Topwal, A. Roy Chaudhuri, D. Choudhury, Origin and tuning of room-temperature multiferroicity in Fe-doped BaTiO3, Phys. Rev. B 101 (2020) 064409.
[70] S. Nagar, K.V. Rao, L. Belova, G. Catalan, J. Hong, J.F. Scott, A.K. Tyagi, O.D. Jayakumar, R. Shukla, Yi-Sheng Liu, J. Guo, Room temperature ferromagnetism and lack of ferroelectricity in thin films of 'Biferroic?' YbCrO3, MRS Proc. 1161 (2009) 1161-I07-04..
[71] K. Agrawal, B. Behera, S.C. Sahoo, S.K. Rout, A. Kumar, P.R. Das, Mn doped multiferroic in Ga0.97Nd0.03FeO3electroceramics, J. Magn. Magn. Mater. 536 (2021) 168121.
[72] J. Nunes-Pereira, V. Sencadas, V. Correia, J.G. Rocha, S. Lanceros-M´endez, Energy harvesting performance of piezoelectric electrospun polymer fibers and polymer/ceramic composites, Sens. Actuators A Phys. 196 (2013) 55–62.
[73] M. Ataur Rahman, B.-Chul Lee, D.-Thach Phan, G.-Sang Chung, Fabrication and characterization of highly efficient flexible energy harvesters using PVDF–graphene nanocomposites, Smart Mater. Struct. 22 (2013) 085017.
[74] Q. Huang, H. Luo, C. Chen, X. Zhou, K. Zhou, D. Zhang, Enhanced energy density in P(VDF-HFP) nanocomposites with gradient dielectric fillers and interfacial polarization, J. Alloy. Compd. 696 (2017) 1220–1227.
[75] J. Wang, J. Hu, Q. Sun, K. Zhu, B. Wen Li, J. Qiu, Dielectric and energy storage performances of PVDF-based composites with colossal permittivitied Nd-doped BaTiO3 nanoparticles as the filler, AIP Adv. 7 (2017) 125104.
[76] S. Godara, B. Kumar, Effect of Ba–Nb co-doping on the structural, dielectric, magnetic and ferroelectric properties of BiFeO3 nanoparticles, Ceram. Int 41 (2015) 6912–6919.
[77] W. Cai, R.L. Gao, L.W. Yao, G. Chen, X.L. Deng, Z.H. Wang, X.L. Cao, F.Q. Wang, Microstructure, enhanced electric and magnetic properties of Bi0.9La0.1FeO3 ceramics prepared by microwave sintering, J. Alloy. Compd. 774 (2019) 61–68.
[78] E.W. Lim, R. Ismail, Conduction mechanism of valence change resistive switching memory: a survey, Electronics 4 (2015) 586–613.
[79] P. Wu, M. Zhang, H. Wang, H. Tang, P. Bass, L. Zhang, Effect of coupling agents on the dielectric properties and energy storage of Ba0.5Sr0.5TiO3/P(VDF-CTFE) nanocomposites, AIP Adv. 7 (2017) 075210.
[80] H. Li, C. Tian, Z. Daniel Deng, Energy harvesting from low frequency applications using piezoelectric materials, Appl. Phys. Rev. 1 (2014) 041301.
[81] P. Costa, J. Nunes-Pereira, N. Pereira, N. Castro, S. Gonçalves, S. Lanceros-Mendez, Recent progress on piezoelectric, pyroelectric, and magnetoelectric polymer-based energy-harvesting devices, Energy Technol. 7 (2019) 1800852.
[82] Q. Guo, G.Z. Cao, I.Y. Shen, Measurements of piezoelectric coefficient d33 of lead zirconate titanate thin films using a mini force hammer, J. Vib. Acoust. 135 (2013) 011003-1.
[83] S.K. Mahadeva, J. Berring, K. Walus, B. Stoeber, Effect of poling time and grid voltage on phase transition and piezoelectricity of poly(vinyledene fluoride) thin films using corona poling, J. Phys. D Appl. Phys. 46 (2013) 285305.
[84] Y. Jiang, Y. Ye, J. Yu, Z. Wu, W. Li, J. Xu, G. Xie, Study of thermally poled and corona charged poly(vinylidene fluoride) films, Polym. Eng. Sci. 47 (2007) 1344–1350.